Insights into the mechanism of substituted metal center regulating the enzymatic activity of Prussian blue analogues for catalytic antioxidation

*Genxiu Zhou[a, #], Qingrong Dong,[a, c, #], Zhi Li[b ,#], Feifei Yang[b], Xiaomei Shen[b, *], Quan Liu[a], Ge Fang[a, *], Cuicui Ge[a, *]*

[a]State Key Laboratory of Radiation Medicine and Protection, School for Radiological and interdisciplinary Sciences (RAD-X) & Collaborative Innovation Center of Radiation Medicine of Jiangsu Higher Education Institutions, Soochow University, Suzhou 215123, China

[b]Key Laboratory of Functional Small Organic Molecule, College of Chemistry and Chemical Engineering, Jiangxi Normal University, Nanchang 330022, China

[c]College of Medical Imaging, Shanxi Medical University, Taiyuan 030001, China

[#]These authors contributed equally to this work

*Corresponding Author(s): shenxm@jxnu.edu.cn; gfang@suda.edu.cn; ccge@suda.edu.cn

Supplement methods

Chemicals

Iron nitrate nonahydrate ($Fe(NO_3)_3 \cdot 9H_2O$, 99.99%), cobalt nitrate hexahydrate ($Co(NO_3)_2 \cdot 6H_2O$, 99.99%), copper acetate monohydrate ($Cu(CH_3COO)_2 \cdot H_2O$, 99.95%), nickel acetate tetrahydrate ($Ni(CH_3COO)_2 \cdot 4H_2O$, 99.0%), potassium ferrocyanide trihydrate ($K_4[Fe(CN)_6] \cdot 3H_2O$, 99.5%), and potassium ferricyanide ($K_3[Fe(CN)_6]$, 99.5%) were purchased from Aladdin (Shanghai, China). Trisodium citrate dihydrate ($Na_3C_6H_5O_7 \cdot 2H_2O$) and citric acid monohydrate ($C_6H_8O_7 \cdot H_2O$, 99.5%) were obtained from Sigma Aldrich (Shanghai, China). Poly(vinylpyrrolidone) (PVP, K30) was purchased from J&K Chemical Technology (Beijing, China). Hydrochloric acid (HCl) and ethanol were acquired from Sinopharm Chemical Reagent Co. (Shanghai, China). Phosphate buffer solution (PBS) was purchased from Sangon Biotech (Shanghai, China). All chemicals were used without further treatment.

Synthesis and characterization of PB NPs and PBAs.

The synthesis of PB NPs (FeFe) were carried out by a hydrothermal method according to the previous literature.[1] In detail, $K_4[Fe(CN)_6]$ (0.01 mmol) and citric acid (5 mmol) were dissolved in 20 mL ultrapure water (Solution A). $Fe(NO_3)_3 \cdot 9H_2O$ (0.05 mmol) and citric acid (5 mmol) were dissolved in another 20 ml ultrapure water (Solution B). Afterwards, solution B was added dropwise into the solution A under magnetic stirring at 60 °C and stirred for further 5 min. After cooled for 30 min, FeFe was collected by centrifugation (9500 rpm, 10 min) and then washed three times with ethanol. Finally, it was dried overnight at 40 ℃ under vacuum. The synthesis of NiFe and CuFe was similar to that of FeFe, while CoFe was synthesized at room temperature using $K_3[Fe(CN)_6]$and $Co(NO_3)_2 \cdot 6H_2O$ as precursors.

Characterization

The morphology of the as-fabricated nanozyme was characterized by Transmission Electron Microscope (TEM, Tecnai G2 spirit BioTwin, FEI, USA). Energy-dispersive X-ray spectroscopy (EDX) elemental mapping was performed using a Talos F200X microscope (FEI, USA). The crystallinity of the nanozyme was characterized by powder X-ray diffraction (PXRD) on a Bruker D8 Advance diffractometer equipped with Cu Kα radiation (λ = 1.5406 Å). The X-ray photoelectron spectroscopy (XPS) analyses were carried out on an X-ray photoelectron spectroscopy (ESCALAB 250Xl, Thermo Fisher Scientific, USA) using monochromatic Al Kα X-Ray source (1486.6 eV). The concentrations of metal element of the as-fabricated nanozymes were quantified by inductively coupled plasma optical emission spectroscopy (ICP-OES, ICAP7200, Thermo Fisher, Germany). Fourier Transform Infrared Spectroscopy (FT-IR) and UV-vis absorption spectra were measured with a Vertex 70 (Bruker, Germany) spectrometer and an UV-vis-near-infrared spectrometer (UV-3600, Shimadzu, Japan), respectively. Electron spin resonance (ESR) measurements were carried out using a Bruker E500 instrument. The settings of experimental parameters were listed as follows: 1 G field modulation, 200 G scan range, microwave frequency, 10 GHz and 100 mW microwave power.

Detection of the antioxidant properties of PB NPs and PBAs

The CAT-like activity of PB NPs and PBAs were detected by measuring the residual H_2O_2 using a Catalase (CAT) assay (Beyotime, China). The rection between H_2O_2 and ammonium molybdate produced a yellow complex with a characteristic absorption peak at 405 nm, which could be detected using a microplate reader (BioTek, USA). In a typical experiment, reagents were added to H_2O solution in the order of PBA nanozymes (final concentration 50 μg/mL) and 300 μL of H_2O_2 (final concentration 0.5

M). Steady-state kinetics assays were conducted at 37 °C in 500 μL of reaction solution (H_2O) with 12.5 μL of PBA nanozyme solution (final concentration 50 μg/mL) as a catalyst and a series of concentrations of H_2O_2 (0.2, 0.4, 0.6, 0.8, 1 mM) as a substrate, respectively. All the Michaelis- Menten constants can be calculated according to the following equation:

$$v = V_{max} * [S]/(K_m + [S])$$

where ν represents the initial velocity and V_{max} is defined as the maximum reaction velocity. [S] is the concentration of H_2O_2, and K_m represents the Michaelis constant.

The SOD-like activity of PB NPs and PBAs were assessed by measuring superoxide anion (O_2•$^-$) using BMPO as a spin trap. O2•$^-$ was produced in the xanthine/XOD system. Taking CuFe PBAs as an example, the samples contained 1 mM BMPO, 5 μg/mL nanozyme, 0.1 U/mL XOD, and 0.5 mM hypoxanthine. Samples were placed in quartz capillary tubes and then ESR spectra were measured after coincubation for 5 min.

CuFe PBAs protect cells against oxidative damage

To verify the cytoprotection effect of CuFe PBAs, the HUVEC cells were incubated in the 96-well cell culture for 24 h with the cell density at 60-80%; then, the medium of cells was replaced by the fresh serum-free medium containing H_2O_2 (final concentration 600 μM) with or without PBAs (final concentration 200 μg/ml). After 2 h incubation, the cell viability was detected using the CCK-8 viability test kit by the microplate reader (BioTek, USA). Intracellular reactive oxygen species (ROS) generation was monitored using 2,7-Dichlorodihydrofluorescein Diacetate (DCFH-DA) as a fluorescent probe. HUVEC cells were exposed to H_2O_2 with or without PBAs (200 μg/mL). After 2 h treatment, cells were washed and incubated with 10 μM DCFH-DA for 30 min. Finally, the intracellular fluorescence signal was measured using a confocal laser microscope

(FV1200, OLYMPUS, Japan).

Electrochemical measurements

Electrochemical measurements were performed on a CHI 600E electrochemical workstation (Shanghai Chenhua Instrument Company, China) in a standard three-electrode configuration, in which silver/silver chloride (Ag/AgCl) and platinum wire were employed as the reference and counter electrodes respectively. A glassy carbon electrode served as the substrate to be deposited with different PBAs for the working electrodes. Phosphate Buffered Saline solution (0.1 mol/L, pH 7.4) was used as the electrolyte. The cyclic voltammogram (CV) curves were collected at a scan rate of 0.1 V s^{-1} in the range from -1.6 to 2 V for 1 cycle.

Computational Details

DFT calculations were performed by Vienna ab initio Simulation Package (VASP).[2-4] The electronic structures were calculated by Generalized gradient approximation (GGA) and Perdew-Burke–Ernzerhof (PBE) of projector augmented wave (PAW) methods.[5, 6] The energy cut-off was set to 400 eV. (001) slabs of MFe with (1 × 1) unit cells were cleaved for FeFe, CuFe, NiFe and CoFe. The vacuum values were set to 15 Å in the vertical directions. The Brillouin zones were sampled with 3 × 3 × 1 Monkhorst-Pack mesh k-point grids.[7] During geometry optimization, conjugated gradient algorithm was used, and all the bottom two layers were frozen and atoms on the other layers were relaxed. For all calculations, the electronic energy and force were required to converge until 10^{-5} eV and 0.01 eV/Å, respectively. Implicit solvent model was implemented by VASPsol.[8, 9] Spin polarization was used for all calculations. The adsorption energy (E_{ads}) of the adsorbate X on the surface was calculated through the following equation:

$$E_{ads} = E_{X/surf} - (E_X + E_{surf})$$

Where $E_{X/surf}$ denotes the total energy of adsorbate adsorption on surface, E_{surf} and E_X represents the energies of isolated bare surface and adsorbate, respectively.

Table S1 The molar ratio of Fe to M(Co, Ni, Cu) in the as-synthesized PB NPs and PBAs.

PBAs	The molar ratio of Fe to M
CoFe	**1:1.79**
NiFe	**1:1.55**
CuFe	**1:1.71**

Table S2 Redox potential (*v vs*. SHE) obtained from the oxidation and reduction peaks observed during cyclic voltammetry (0.1 $V \cdot s^{-1}$) of PBAs.

Cation	E_{PA} (V)	E_{PC} (V)	E1/2 (V VS. SHE)
FeFe	0.90	0.69	0.79
CoFe	0.75	0.64	0.69
NiFe	0.60	0.51	0.55
CuFe	0.40, 0.55	0.11, 0.30	0.26

Table S3 The magnetic moment (μ_B) of the metal atoms in the MFe (M= Fe, Co, Ni, Cu) bulks.

Species	Atom position	Magnetic moment (μ_B)
FeFe	Fe_N	0.98
	Fe_C	0.96
CoFe	Co_N	0.14
	Fe_C	0.78
NiFe	Ni_N	0.31
	Fe_C	0.42
CuFe	Cu_N	0.95
	Fe_C	1.02

Table S4 The magnetic moment (μ_B) of the metal atoms in the MFe(001) (M= Fe, Co, Ni, Cu) slabs.

Species	Atom position	Magnetic moment (μ_B)
FeFe	$^{S}Fe_N$	2.35
	$^{S}Fe_C$	0.45
	$^{B}Fe_N$	1.43
	$^{B}Fe_C$	1.10
CoFe	$^{S}Co_N$	0.15
	$^{B}Co_N$	0.11
	$^{S}Fe_C$	0.25
	$^{B}Fe_C$	1.21
NiFe	$^{S}Ni_N$	0.49
	$^{B}Ni_N$	0.12
	$^{S}Fe_C$	0.33
	$^{B}Fe_C$	0.93
CuFe	$^{S}Cu_N$	0.64
	$^{B}Cu_N$	0.86
	$^{S}Fe_C$	0.99
	$^{B}Fe_C$	1.53

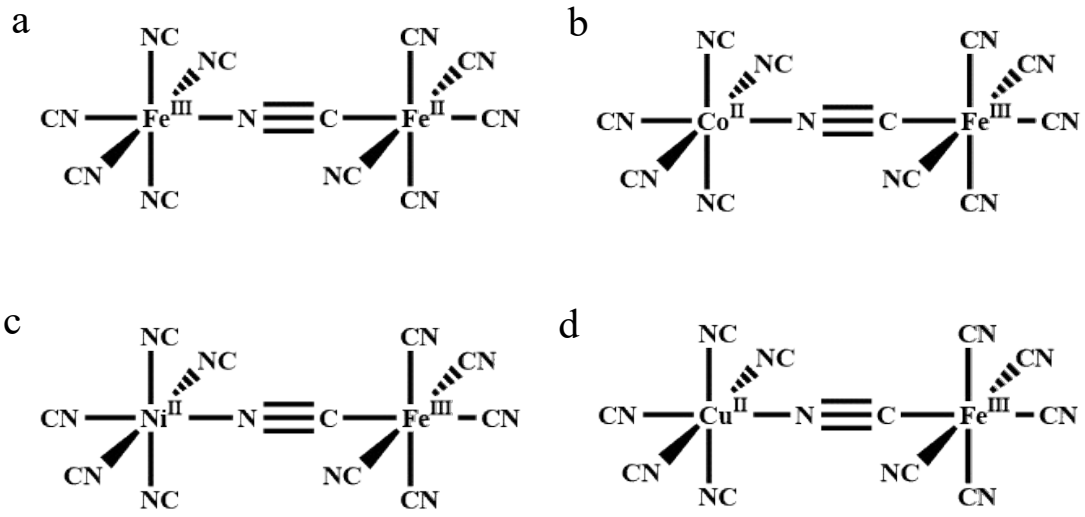

Figure S1 Coordination structures of (a) FeFe, (b) CoFe, (c)NiFe, and (d) CuFe PBAs.

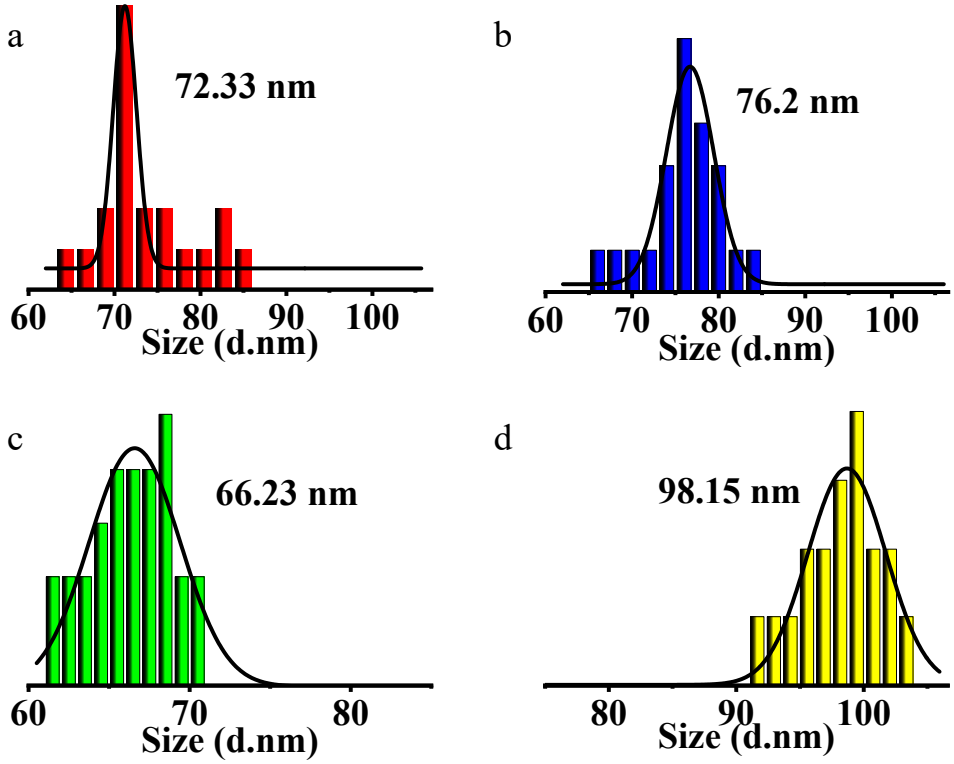

Figure S2 Size distribution of (a) FeFe, (b) CoFe, (c)NiFe, and (d) CuFe PBAs analyzed by the Nano Measure software.

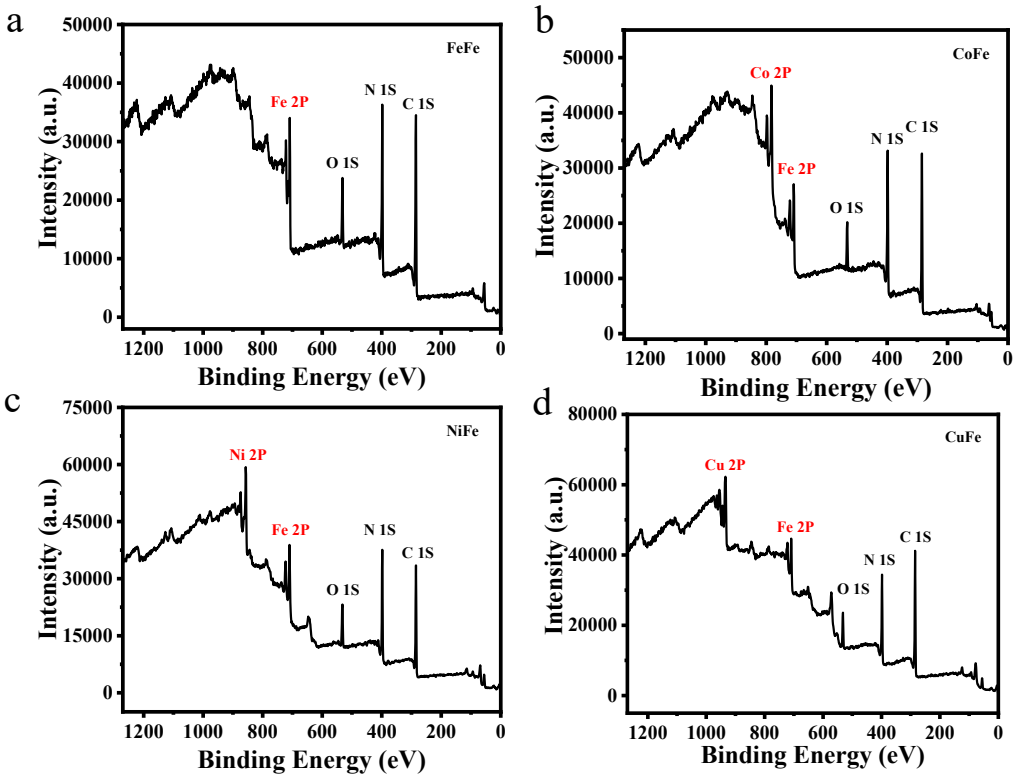

Figure S3 The XPS spectra of (a) FeFe, (b) CoFe, (c) NiFe, and (d) CuFe PBAs.

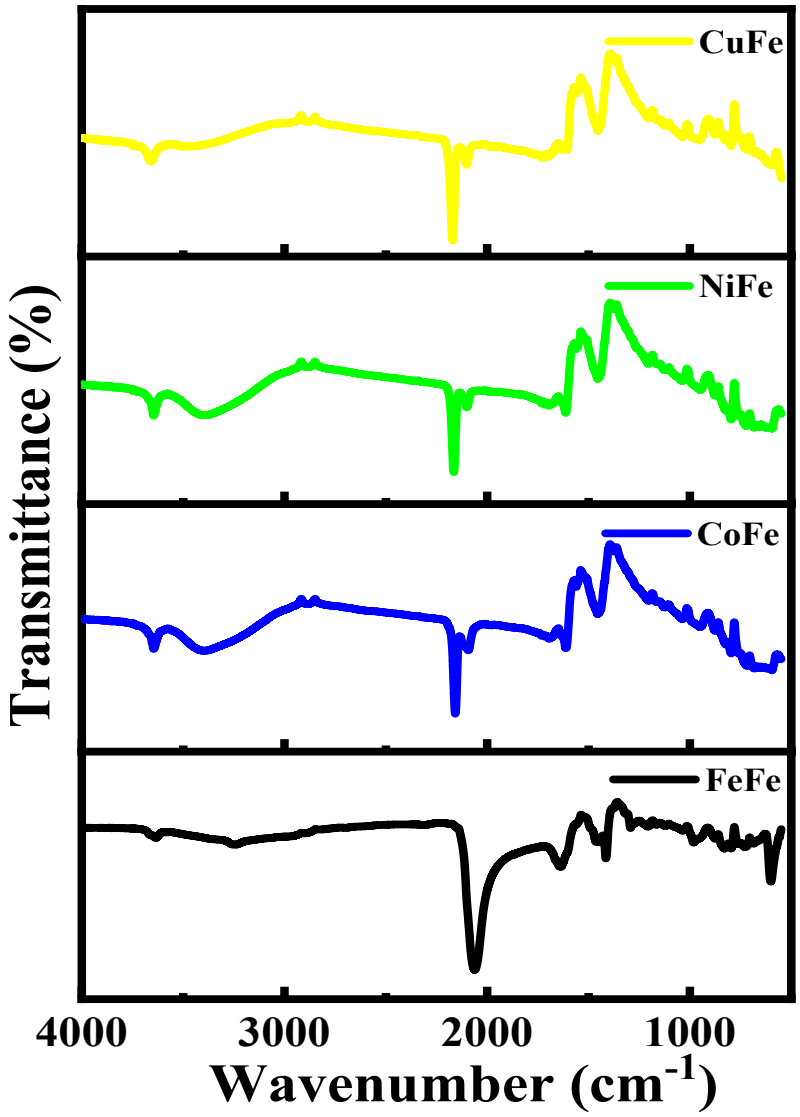

Figure S4 FTIR spectra of (a) FeFe, (b) CoFe, (c) NiFe, and (d) CuFe PBAs.

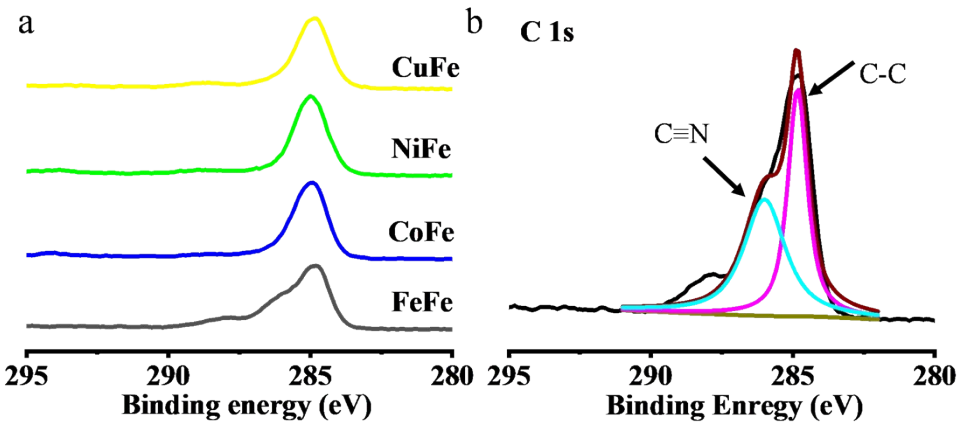

Figure S5 (a) High-resolution C 1S XPS spectra of PBAs. (b) The analysis on the C 1S XPS spectrum of FeFe.

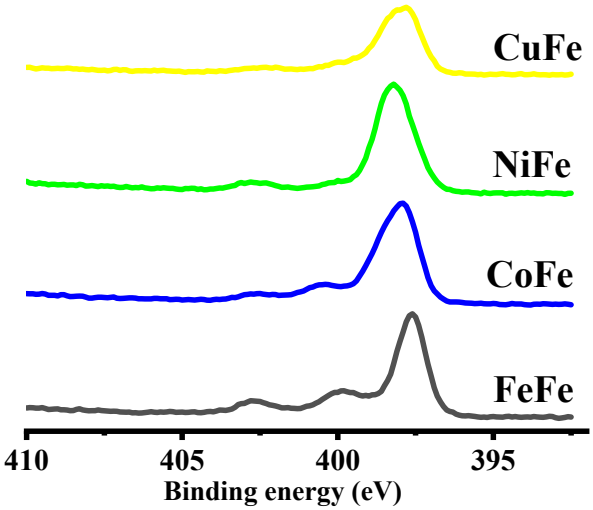

Figure S6 High-resolution N 1S XPS spectra of PBAs.

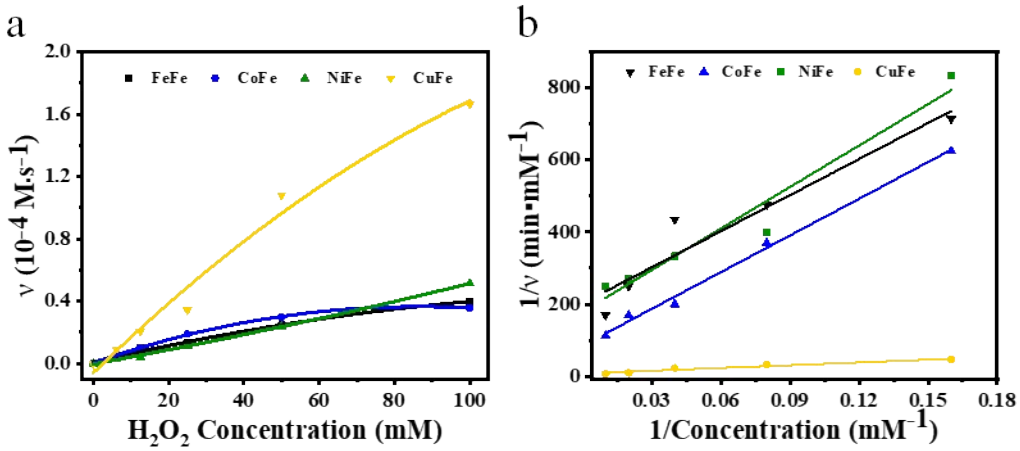

Figure S7 (a) Characterization of the catalytic kinetics of PB and PBAs in the presence of varying H_2O_2 concentration. (b) Double-reciprocal plots of activity of PB and PBAs.

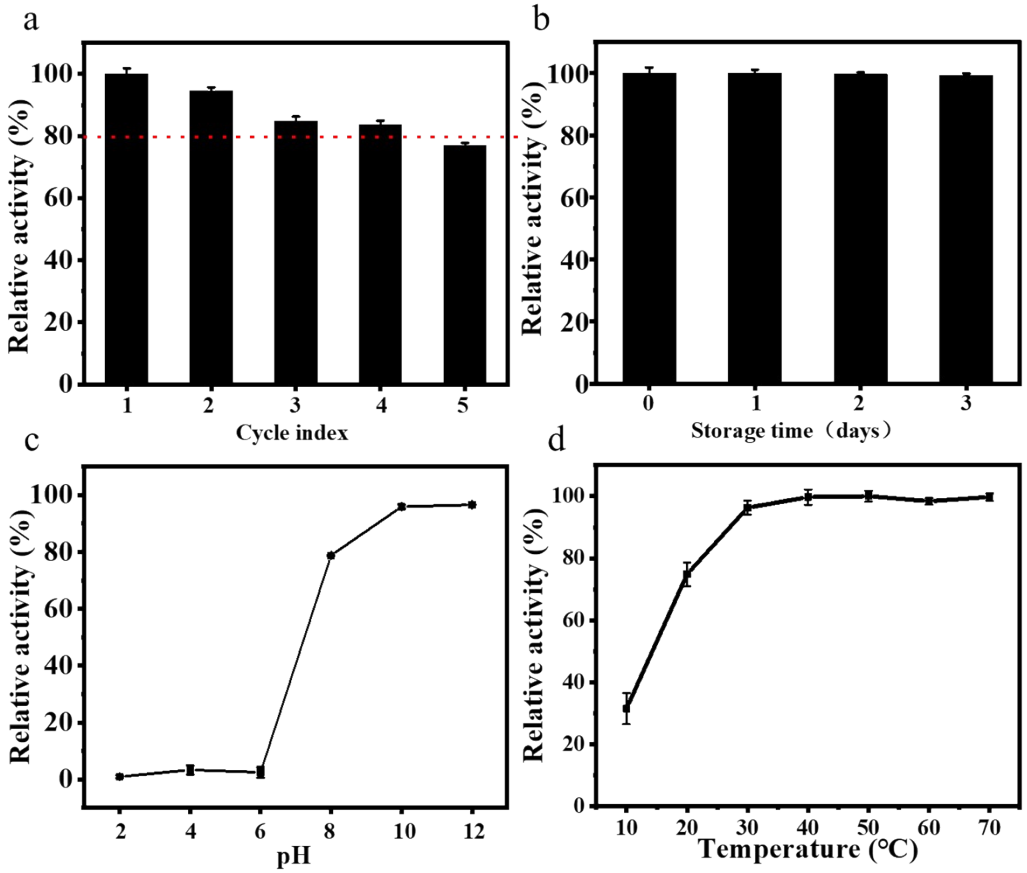

Figure S8 CAT-like property of the CuFe with different cycle numbers(a) and storage time(b) and under different pH (c) and temperatures (d).

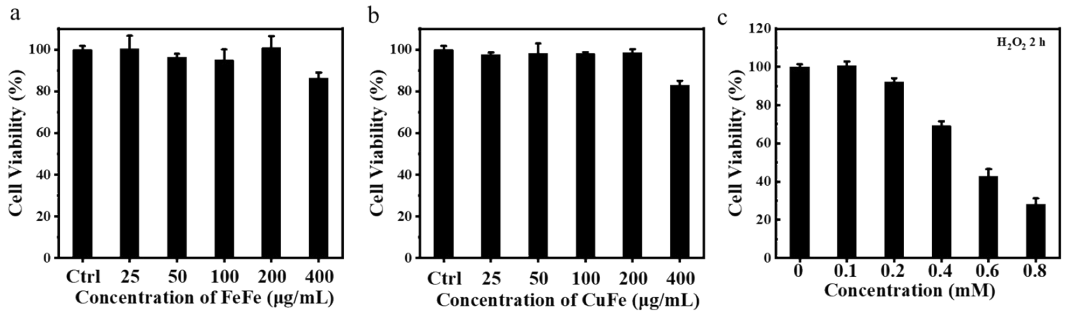

Figure S9 Cytotoxicity of FeFe (a), CuFe (b) PBAs and H_2O_2on HUVECs in serum-free media for 24 h.

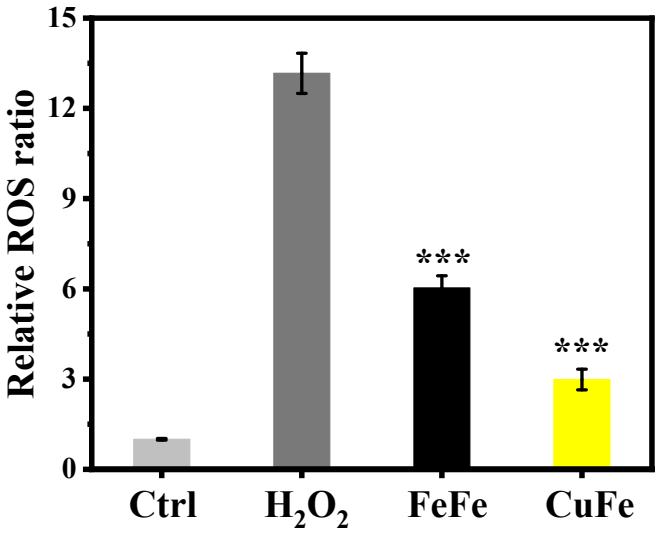

Figure S10 Quantitative analysis of ROS levels using image J software. Data are shown as mean ± SD (n = 3). *p<0.05, **p<0.01, ***p<0.001.

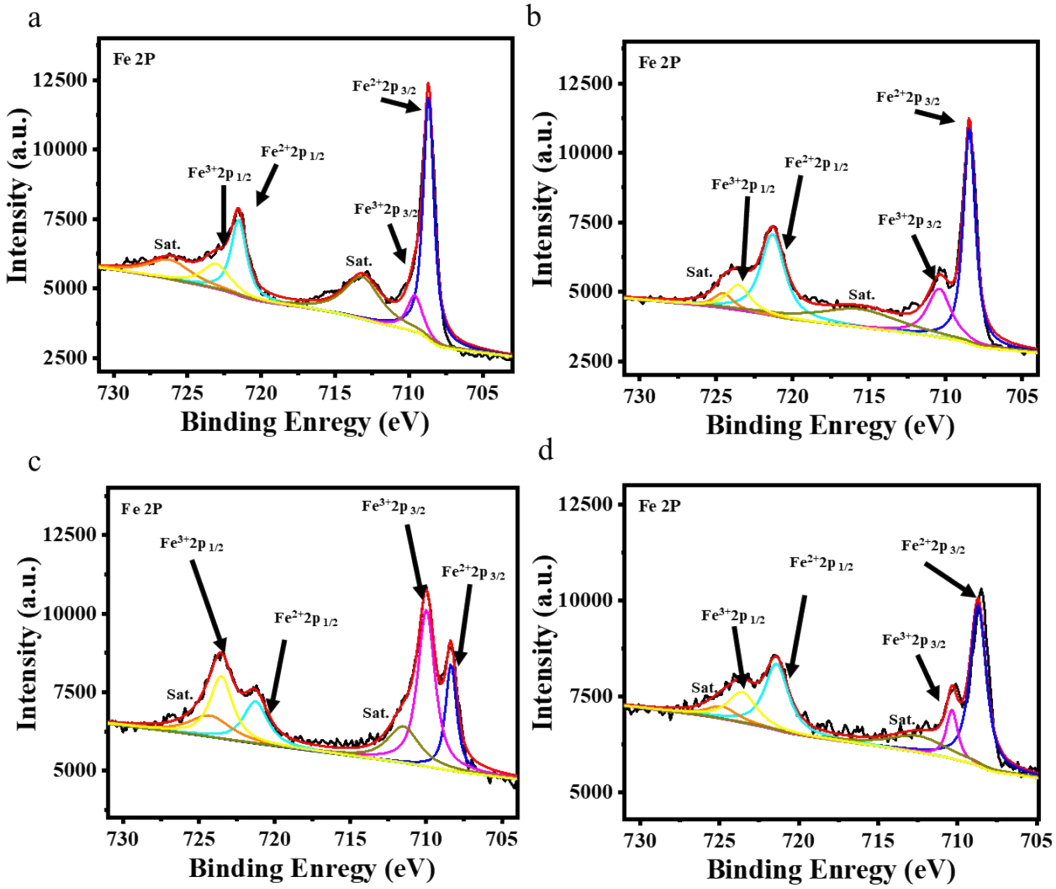

Figure S11 The high resolution XPS spectra of Fe 2p for (a)PB, (b)CoFe, (c)NiFe and (d)CuFe PBAs.

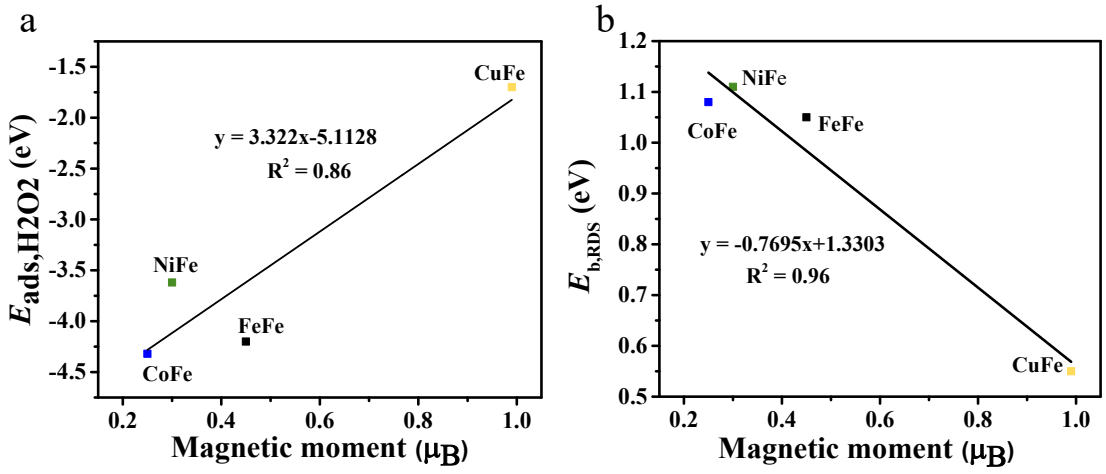

Figure S12 The relationship between the Fe_C magnetic moment and (a) H_2O_2 adsorption energy. (b) The energy barrier of the rate-determining step.

References

1. Chen, J.; Wang, Q.; Huang, L.; Zhang, H.; Rong, K.; Zhang, H.; Dong, S. *Nano Research* **2018,** 11, (9), 4905-4913.

2. Kresse, G.; Joubert, D. *Physical Review B* **1999,** 59, (3), 1758-1775.

3. Kresse, G.; Furthmuller, J. *Computational Materials Science* **1996,** 6, (1), 15-50.

4. Kresse, G.; Furthmuller, J. *Physical Review B* **1996,** 54, (16), 11169-11186.

5. Perdew, J. P.; Burke, K.; Ernzerhof, M. *Physical review letters* **1996,** 77, (18), 3865-3868.

6. Blöchl, P. E. *Physical Review B* **1994,** 50, (24), 17953-17979.

7. Methfessel, M.; Paxton, A. T. *Physical Review B* **1989,** 40, (6), 3616-3621.

8. Mathew, K.; Kolluru, V. S. C.; Mula, S.; Steinmann, S. N.; Hennig, R. G. *The Journal of chemical physics* **2019,** 151, (23), 234101.

9. Mathew, K.; Sundararaman, R.; Letchworth-Weaver, K.; Arias, T. A.; Hennig, R. G. *The Journal of chemical physics* **2014,** 140, (8), 084106.